

SELF-REGULATED GROWTH OF SUPERMASSIVE BLACK HOLES IN GALAXIES AS THE ORIGIN OF THE OPTICAL AND X-RAY LUMINOSITY FUNCTIONS OF QUASARS

J. STUART B. WYITHE AND ABRAHAM LOEB
 swyithe@isis.ph.unimelb.edu.au; loeb@sns.ias.edu

Draft version November 7, 2018

ABSTRACT

We postulate that supermassive black-holes grow in the centers of galaxies until they unbind the galactic gas that feeds them. We show that the corresponding self-regulation condition yields a correlation between black-hole mass (M_{bh}) and galaxy velocity dispersion (σ) as inferred in the local universe, and recovers the observed optical and X-ray luminosity functions of quasars at redshifts up to $z \sim 6$ based on the hierarchical evolution of galaxy halos in a Λ CDM cosmology. With only one free parameter and a simple algorithm, our model yields the observed evolution in the number density of optically bright or X-ray faint quasars between $2 \lesssim z \lesssim 6$ across 3 orders of magnitude in bolometric luminosity and 3 orders of magnitude in comoving density per logarithm of luminosity. The self-regulation condition identifies the dynamical time of galactic disks during the epoch of peak quasar activity ($z \sim 2.5$) as the origin of the inferred characteristic quasar lifetime of $\sim 10^7$ years. Since the lifetime becomes comparable to the Salpeter e -folding time at this epoch, the model also implies that the $M_{\text{bh}} - \sigma$ relation is a product of feedback regulated accretion during the peak of quasar activity. The mass-density in black-holes accreted by that time is consistent with the local black-hole mass density $\rho_{\text{bh}} \sim (2.3_{-1.5}^{+4.0}) \times 10^5 M_{\odot} \text{Mpc}^{-3}$, which we have computed by combining the $M_{\text{bh}} - \sigma$ relation with the *measured* velocity dispersion function of SDSS galaxies (Sheth et al. 2003). Comparison of the local black-hole mass-function with that inferred from combining the feedback-relation with the halo mass-function suggests that most massive ($> 10^9 M_{\odot}$) black-holes may have already been in place by $z \sim 6$. Applying a similar self-regulation principle to supernova-driven winds from starbursts, we find that the ratio between the black hole mass and the stellar mass of galactic spheroids increases with redshift as $(1+z)^{3/2}$ although the $M_{\text{bh}} - \sigma$ relation is redshift-independent.

Subject headings: black-hole physics - quasars: general

1. INTRODUCTION

It has long been recognized that the formation processes of supermassive black-holes (BHs) and stars may be self-regulating (Dekel & Silk 1986; Silk & Rees 1998), since the amount of energy released by quasars and stars can exceed the binding energy of the gas clouds in which they are born. Indeed, the stellar and central BH masses of galaxies show striking correlations with the depth of the gravitational potential well of their hosts. These phenomenological correlations take the form of the mass-velocity dispersion correlation for BHs (Merritt & Ferrarese 2001; Tremaine et al. 2002) and the Tully-Fisher (1977) and Faber-Jackson (1976) relations for stars in the present-day universe.

In this paper we explore the self-limiting growth of the BH and stellar masses of galaxies as a function of cosmic time, and investigate the consequences for the quasar luminosity function. Recent work suggests that the kinetic output of quasars may be comparable to their radiative output (see §2.1.1 in Furlanetto & Loeb 2001; Begelman 2003). Our simple approach postulates that growth stops when the energy released by these sources exceeds the binding energy of the gas within their host galaxies after one dynamical time of the gas reservoir. Using the redshift-dependent abundance of galactic halos as a function of potential depth in a Λ CDM cosmology, we demon-

strate that this simple approach describes the luminosity function of quasars in optical and X-ray bands. We adopt the WMAP set of cosmological parameters (Bennett et al. 2003), namely mass density parameters of $\Omega_m = 0.27$ in matter, $\Omega_b = 0.044$ in baryons, $\Omega_{\Lambda} = 0.73$ in a cosmological constant, a Hubble constant of $H_0 = 71 \text{ km s}^{-1} \text{ Mpc}^{-1}$, an rms amplitude of $\sigma_8 = 0.84$ for mass density fluctuations in a sphere of radius $8h^{-1} \text{ Mpc}$, and a primordial power-spectrum with a power-law index $n = 1$.

We begin the paper with a discussion of the regulation of BH growth by feedback during luminous quasar phases (§ 2) and then discuss the implications for modeling of the optical (§ 3.1) and X-ray (§ 3.2) luminosity functions of quasars, including the number counts of high-redshift X-ray quasars (§ 3.3). We subsequently compute the mass accreted into BHs during luminous quasar phases (§ 4) and compare this to the local density in BHs (§ 5), which we compute using the measured velocity dispersion function of *Sloan Digital Sky Survey* (SDSS) galaxies (Sheth et al. 2003). In § 5 we also demonstrate that the most massive BHs were already in place at high redshift. We then show in § 6 and § 7 that while the $M_{\text{bh}} - \sigma$ relation is redshift-independent, the ratio of BH mass to stellar mass within galaxies should increase with increasing redshift if both are regulated by a similar feedback process. Finally we compare our findings with some previous work in § 8

¹ The University of Melbourne, Parkville, Vic, Australia

² Institute for Advanced Study, Princeton, NJ 08540

³ Guggenheim Fellow; on leave from the Astronomy Department, Harvard University, Cambridge, MA 02138

and summarize our main conclusions in § 9.

2. FEEDBACK AND THE GROWTH OF GALACTIC BLACK-HOLES

The growth of a supermassive BH is expected to be accelerated during a galaxy merger, when cold gas is driven to the center of the merger remnant (Mihos & Hernquist 1994; Hernquist & Mihos 1995). Yu & Tremaine (2002) have found that the local mass density in BHs is consistent with the integrated luminosity density of quasars if the mean radiative efficiency of the accreting material is $\epsilon_{\text{rad}} \sim 8\%$; moreover, they concluded that about half the current BH mass density was accreted near the Eddington rate at redshift $z \gtrsim 2$. It is natural to expect that a quasar shining at its limiting Eddington luminosity could generate a powerful galactic wind and eventually terminate the accretion process that feeds it.

Indeed, Silk & Rees (1998) pointed out that winds from quasars could generate self-regulating outflows in the surrounding gas, if the energy in the outflow liberates as much as the binding energy of the gas in a dynamical time. For a quasar output power that scales as the Eddington limiting luminosity, this condition leads to a power-law scaling of the BH mass with halo velocity dispersion, $M_{\text{bh}} \propto \sigma^5$. This scaling was used by Haehnelt, Natarajan & Rees (1998) to demonstrate consistency between the density of quasars at $z \sim 3$ and the time derivative of the Press-Schechter mass-function for a quasar lifetime that is comparable with the Salpeter time (the e -folding time of the BH mass), $\sim 2.4 \times 10^7 (\epsilon_{\text{rad}}/0.06)$ yr. Here we extend an earlier model (Wyithe & Loeb 2002) to include feedback limited BH growth within the context of hierarchical merging in a Λ CDM cosmology. We compare our model with the most recent data for the space density of high redshift quasars at both optical and X-ray wavelengths.

We assume that following a merger, a BH shines at a fraction η of its Eddington luminosity ($\propto M_{\text{bh}}$) returning fraction F_{q} of this energy⁴ to the galactic gas. The quasar will unbind the galactic gas if it supplies as much as the gravitational binding energy of the gas over the time it takes the gas to respond dynamically to this energy injection, t_{dyn} . The cold gas is usually located in a disk with a characteristic radius $(\lambda/\sqrt{2})r_{\text{vir}} \sim 0.035r_{\text{vir}}$ (Mo, Mao & White 1998), and hence a dynamical time⁵ of $t_{\text{dyn}} \sim 0.035r_{\text{vir}}/v_{\text{c}}$. Here $\lambda \sim 0.05$ is the spin parameter, r_{vir} is the virial radius, and v_{c} is the circular velocity of the galactic halo⁶ (Barkana & Loeb 2001),

$$v_{\text{c}} = 245 \left(\frac{M_{\text{halo}}}{10^{12} M_{\odot}} \right)^{1/3} [\xi(z)]^{1/6} \left(\frac{1+z}{3} \right)^{1/2} \text{ km s}^{-1}, \quad (1)$$

where $\xi(z)$ is close to unity and defined as $\xi \equiv [(\Omega_m/\Omega_m^z)(\Delta_c/18\pi^2)]$, $\Omega_m^z \equiv [1 + (\Omega_{\Lambda}/\Omega_m)(1+z)^{-3}]^{-1}$, $\Delta_c = 18\pi^2 + 82d - 39d^2$, and $d = \Omega_m^z - 1$ (see Barkana & Loeb 2001 for more details). The value of F_{q} should be of order unity if the gas traps much of the quasar output energy without radiating it away (Begelman 2003). The

self-regulation condition is then,

$$\eta L_{\text{Edd},\odot} M_{\text{bh}} F_{\text{q}} = \frac{\epsilon_{\text{rad}} \delta M_{\text{bh}} c^2}{t_{\text{dyn}}} F_{\text{q}} = \frac{\frac{1}{2} \Omega_m M_{\text{halo}} v_{\text{c}}^2}{t_{\text{dyn}}}, \quad (2)$$

where M_{halo} is the halo mass, δM_{bh} is the mass accreted and $L_{\text{Edd},\odot}$ is the Eddington luminosity per unit mass (M_{\odot}). Note that we assume (as appropriate at high redshifts) that all the gas within a galactic halo cools on a time much shorter than the Hubble time. Our primary objective is to show that this condition is sufficient to describe the quasar luminosity function at $z \gtrsim 2$ (before groups and clusters of galaxies become prominent). Equation (2) implies $M_{\text{bh}} \propto v_{\text{c}}^5$ as inferred for galactic halos in the local universe (Ferrarese 2002). The index of 5 is larger than the 4-4.5 inferred from the local $M_{\text{bh}} - \sigma$ relation (Merritt & Ferrarese 2001; Tremaine et al. 2002), the difference having its origin in the observation that the $v_{\text{c}} - \sigma$ relation is shallower than linear (Ferrarese 2002). The index of 5 is also larger than presented in the recent work of Baes, Buyle, Hau & Dejonghe (2003), with the difference having its origin in the uncertainty in the slope of the $M_{\text{bh}} - \sigma$ relation. Feedback regulated growth implies that the $M_{\text{bh}} - v_{\text{c}}$ relation is independent of redshift,

$$M_{\text{bh}} = 1.9 \times 10^8 M_{\odot} \left(\frac{\eta F_{\text{q}}}{0.07} \right) \left(\frac{v_{\text{c}}}{350 \text{ km s}^{-1}} \right)^5. \quad (3)$$

The redshift independence is consistent with the recent results of Shields et al. (2002). Using quasars out to $z \sim 3$, they demonstrated that the $M_{\text{bh}} - \sigma$ relation does not evolve with redshift. The resulting relation between BH and halo mass may be written as

$$\begin{aligned} M_{\text{bh}}(M_{\text{halo}}, z) &= \epsilon M_{\text{halo}} \\ &= \epsilon_o M_{\text{halo}} \left(\frac{M_{\text{halo}}}{10^{12} M_{\odot}} \right)^{\frac{2}{3}} [\xi(z)]^{\frac{5}{6}} (1+z)^{\frac{5}{2}}. \end{aligned} \quad (4)$$

Assuming $\eta = 1$ as suggested by observations of low and high-redshift quasars (Floyd 2003; Willott, McLure & Jarvis 2003), we can compute the normalization in equation (4) from equation (2). The only adjustable parameter in our model if $\eta \sim 1$ is F_{q} . If the BH growth was mostly complete by a redshift $z \sim 1-2$ (Yu & Tremaine 2002) so that the local BH masses reflect the limiting values at that redshift, then a value of $\epsilon_o = 10^{-5.7}$ is consistent with BH masses that are measured locally (Ferrarese 2002). This implies a value of $F_{\text{q}} = 0.07$.

Modification of the simple scheme described above would be required if cooling of the gas heated by the outflow is important so that additional energy is required to unbind the gas. The factor required could be as large as c/v_{c} based on momentum conservation (Begelman 2003), with the resulting dependence $M_{\text{bh}} \propto v_{\text{c}}^4$. This relation is shallower than observed. The importance of cooling can be evaluated by estimating the cooling time for virialized gas. The cooling rate for primordial gas of temperature $T_{\text{vir}} \gtrsim 10^6 \text{ K}$ and proton density $1.2 \times 10^{-3} [(1+z)/3]^3 \text{ cm}^{-3}$ (typical for a virialized halo)

⁴ If the energy output of the quasar is communicated to the galaxy through a wind with an outflow velocity that is not much larger than the escape velocity of the halo, then momentum conservation leads to the same condition as equation (2).

⁵ We assume that gas can be driven towards the black hole during the merger. Such accretion is communicated over the characteristic dynamical time r/v (as appropriate for a radial orbit) rather than $2\pi r/v$ (as appropriate for a circular orbit).

⁶ One inaccuracy in our modeling is that we assume dark matter halos to be singular isothermal spheres, while an NFW profile gives a lower v_{c} at the disk radius than at r_{vir} . We ignore this difference because galaxies appear to have nearly flat rotation curves in practice.

is $\Lambda \sim 8.7 \times 10^{-30} [(1+z)/3]^6 (T_{\text{vir}}/10^6 \text{K})^{1/2} \text{erg cm}^{-3} \text{s}^{-1}$ (Barkana & Loeb 2001). We have adopted a cooling rate that increases as \sqrt{T} above $T_{\text{vir}} = 10^6 \text{K}$ assuming that it is dominated by bremsstrahlung at higher temperatures. The thermal energy per unit volume in this gas is $E \sim 5 \times 10^{-13} [(1+z)/3]^3 (T_{\text{vir}}/10^6 \text{K}) \text{erg cm}^{-3}$. The cooling time for virialized gas is therefore

$$t_{\text{cool}} \sim \frac{E}{\Lambda} \sim 2 \times 10^9 \left(\frac{1+z}{3} \right)^{-3} \left(\frac{T_{\text{vir}}}{10^6 \text{K}} \right)^{1/2} \text{yr}, \quad (5)$$

where the virial temperature is given by (Barkana & Loeb 2001),

$$T_{\text{vir}} = 2.2 \times 10^6 \left(\frac{M_{\text{halo}}}{10^{12} M_{\odot}} \right)^{2/3} [\xi(z)]^{1/3} \left(\frac{1+z}{3} \right) \text{K}. \quad (6)$$

The cooling time should be compared with the characteristic lifetime of the quasar, which our model relates to the dynamical time of the galactic disk,

$$t_{\text{dyn}} = 0.035 \frac{r_{\text{vir}}}{v_c} = 10^7 [\xi(z)]^{-1/2} \left(\frac{1+z}{3} \right)^{-3/2} \text{yr}. \quad (7)$$

Thus we expect the halo cooling time to be longer than t_{dyn} in the range of redshifts and virial temperatures relevant for bright quasars. As soon as the gas is expelled into the galactic halo and is heated beyond its virial temperature, it will not be able to cool during the quasar activity. Hence we assume that accretion is halted as soon as the quasar supplies the entire galactic gas with more than its binding energy.

3. MODELING THE QUASAR LUMINOSITY FUNCTION

The peak in the quasar luminosity function at $z \sim 2$ coincides with the transition of the characteristic mass scale of collapsed halos through the mass range of interest for the $M_{\text{bh}} - M_{\text{halo}}$ relation. In the present-day universe, the characteristic $1-\sigma$ mass scale is $\sim 10^{13}-10^{14} M_{\odot}$. However galaxies reflect the characteristic mass scale of $\sim 10^{11}-10^{12} M_{\odot}$ at $z \sim 2$, and combine to make groups and clusters rather than super-galaxies today. It may be that galaxies of this characteristic size do not form due to prevention of cooling through conduction or the removal of cold gas from halos (e.g. Benson et al. 2003), or because the stars in giant ellipticals have already formed and expelled the surrounding gas at $z \sim 6$ (Loeb & Peebles 2003). The excursion set formalism describes the rate of galaxy mergers near the characteristic mass at times earlier than $z \sim 2$, but describes the formation rate of groups and clusters near the characteristic mass at later times. The evolution of the bright end of the quasar luminosity function is therefore only tractable to analytic descriptions at early times ($z \gtrsim 2$), while the faint end should be tractable at all redshifts. Since the observed quasar luminosity function implies that around half the mass in BHs was accreted before $z \sim 2$, the $M_{\text{bh}} - M_{\text{halo}}$ relation should be evident in the bright end of the quasar luminosity function at $z \gtrsim 2-3$. We now demonstrate that this is indeed the case.

⁷ Our model does not account for the population of obscured quasars (Fabian 2003). We implicitly assume that the powerful quasars detected at high redshifts are capable of removing any surrounding gaseous torus that may obscure them, since they release sufficient energy to unbind the gas within the entire host galaxy.

3.1. The optical luminosity function

We model the quasar luminosity function assuming that quasar activity follows major galaxy mergers (mass ratios greater than 3) during which BHs coalesce (Kauffmann & Haehnelt 2000). A linear relation between BH mass and halo mass ($M_{\text{bh}} \propto v_c^3$) would be a natural consequence of BH growth that is dominated by coalescence (Haehnelt et al. 1998). However, a nonlinear relation must result from significant mass accretion during the active quasar phase as found by Yu & Tremaine (2002).

Our approach is based on the formalism described in Wyithe & Loeb (2002). Each quasar is assumed to shine at its Eddington luminosity over a lifetime t_q . The quasar light curve may therefore be written as

$$f(t) = \frac{L_{\text{Edd,B}}}{M_{\text{bh}}} \Theta(t_q - t). \quad (8)$$

where $L_{\text{Edd,B}} = 5.73 \times 10^3 M_{\text{bh}} L_{\odot}$ is the Eddington luminosity in the B-band of a BH with mass M_{bh} in solar masses. The quasar luminosity function (comoving number density of quasars per B-band luminosity L_B) is then

$$\begin{aligned} \Psi(L_B, z) = & \int_0^{\infty} dM_{\text{bh}} \int_{0.25\epsilon M_{\text{halo}}}^{0.5\epsilon M_{\text{halo}}} d\Delta M_{\text{bh}} \int_z^{\infty} dz' \frac{dn_{\text{bh}}}{dM} \Big|_{M=M_{\text{bh}}-\Delta M_{\text{bh}}} \\ & \times \frac{d^2 N_{\text{merge}}}{d\Delta M_{\text{bh}} dt'} \Big|_{M_{\text{bh}}-\Delta M_{\text{bh}}} \frac{dt'}{dz'} \delta[L_B - M_{\text{bh}} f(t_z - t')], \quad (9) \end{aligned}$$

where $\frac{dn_{\text{bh}}}{dM_{\text{bh}}}$ and $\frac{d^2 N_{\text{merge}}}{d\Delta M_{\text{bh}} dt'}$ are the mass function and merger rate for BHs respectively, t_z is the cosmic time at redshift z , and $\delta(x)$ is the Dirac delta function. Integrating over M_{bh} we find

$$\begin{aligned} \Psi(L_B, z) = & \int_{0.25 M_{\text{halo}}}^{0.5 M_{\text{halo}}} d\Delta M_{\text{halo}} \int_{a_{\text{min}} = \frac{1}{1+z_{\text{form}}}}^{a = \frac{1}{1+z}} da \frac{dn_{\text{ps}}}{dM} \Big|_{M=M_{\text{halo}}-\Delta M_{\text{halo}}} \\ & \times \frac{d^2 N_{\text{merge}}}{d\Delta M_{\text{halo}} dt} \Big|_{M_{\text{halo}}-\Delta M_{\text{halo}}} \frac{3}{5\epsilon} \frac{dt}{da} \frac{M_{\text{bh}}}{L_{\text{Edd,B}}}, \quad (10) \end{aligned}$$

where $a = 1/(1+z)$ is the scale factor, z_{form} is the formation redshift of the quasar, and we have used the relation between black-hole and halo mass. Evaluation of this expression requires the number of mergers of halos of mass between ΔM and $\Delta M + d\Delta M$ with halos of mass M , $\frac{d^2 N_{\text{merge}}}{d\Delta M_{\text{halo}} dt} \Big|_{M_{\text{halo}}}$ (Lacey & Cole 1993), as well as the co-moving density of halos with mass M , $\frac{dn_{\text{ps}}}{dM_{\text{halo}}}$ (Press & Schechter 1974).

Assuming $t_q \ll H^{-1}(z)$, we then obtain $a - a_{\text{min}} = \frac{da}{dt} t_q$, yielding the luminosity function⁷

$$\begin{aligned} \Psi(L, z) = & \int_{0.25 M_{\text{halo}}}^{0.5 M_{\text{halo}}} d\Delta M_{\text{halo}} \frac{3}{5\epsilon} \frac{t_q}{5.73 \times 10^3 L_{\odot} M_{\odot}^{-1}} \\ & \times \frac{dn_{\text{ps}}}{dM} \Big|_{M=M_{\text{halo}}-\Delta M_{\text{halo}}} \frac{d^2 N_{\text{merge}}}{d\Delta M_{\text{halo}} dt} \Big|_{M_{\text{halo}}-\Delta M_{\text{halo}}} \quad (11) \end{aligned}$$

where we have used $M_{\text{bh}} = L_{\text{Edd,B}} / (5.73 \times 10^3 L_{\odot} M_{\odot}^{-1})$. We impose a lower cutoff on the mass of halos that can contain a quasar. Following reionization, the cutoff mass

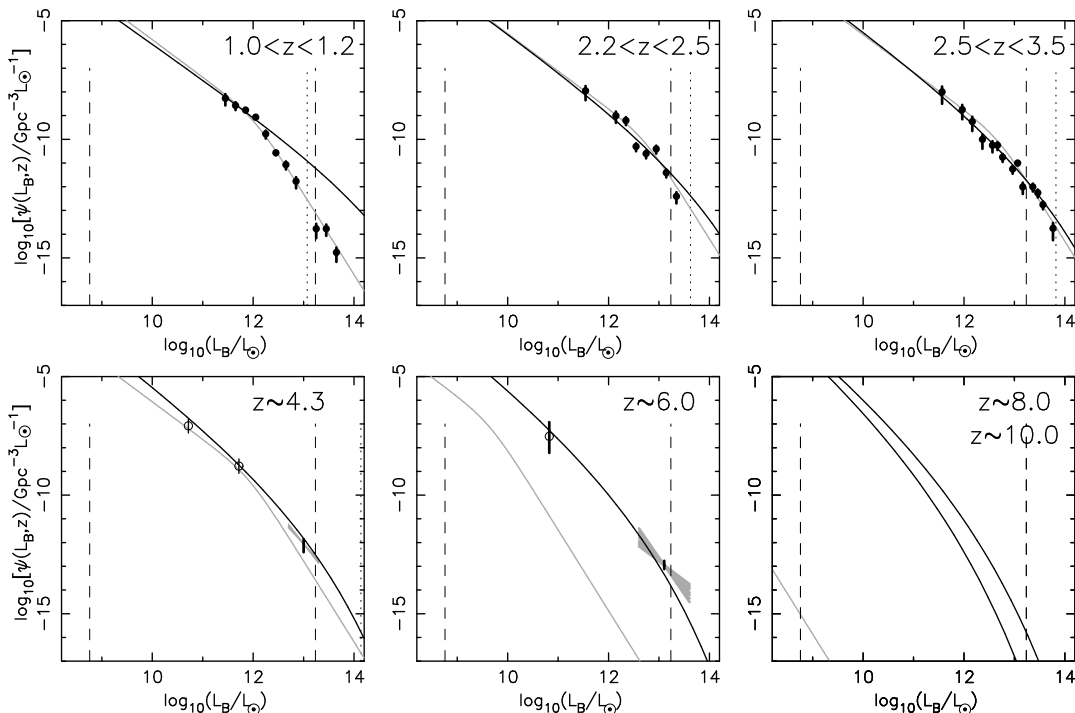


FIG. 1.— Comparison of the observed and model luminosity functions. The data points at $z \lesssim 4$ are summarized in Pei (1995), while the light lines show the double power-law fit to the 2dF quasar luminosity function (Boyle et al. 2000). At $z \sim 4.3$ and $z \sim 6.0$ the data is from Fan et al. (2001a;2001b;2003). The grey regions show the $1\text{-}\sigma$ range of logarithmic slope ($[-2.25, -3.75]$ at $z \sim 4.3$ and $[-1.6, -3.1]$ at $z \sim 6.0$), and the vertical bars show the uncertainty in the normalization. The open circles show data points converted from the X-ray luminosity function (Barger et al. 2003) of low luminosity quasars using the median quasar spectral energy distribution. In each panel the vertical dashed lines correspond to the Eddington luminosities of BHs bracketing the observed range of the $M_{\text{bh}}\text{-}v_c$ relation, and the vertical dotted line corresponds to a BH in a $10^{13.5} M_{\odot}$ galaxy.

corresponds to the Jeans mass in an ionized intergalactic medium (IGM), i.e. a virial temperature of $\sim 2.5 \times 10^5 \text{K}$ (Barkana & Loeb 2001). Equation (2) implies that the quasar lifetime should be identified with the dynamical time of a galactic disk, $t_q \sim t_{\text{dyn}}$, where t_{dyn} is given in equation (7).

We show a comparison between the observed and theoretical luminosity functions in Fig. 1. The model successfully describes the known features of the optical quasar luminosity function at $z \gtrsim 2$. We also show on these plots the range of quasar luminosities corresponding to BH masses observed locally to define the $M_{\text{bh}} - M_{\text{halo}}$ relation (dashed lines). The black holes powering quasars at $z \sim 2$ are at the upper end of the mass range of the BHs observed locally. As discussed above, the $M_{\text{bh}} - M_{\text{halo}}$ relation is obeyed locally by galaxies, but not by groups or clusters of galaxies inside of which the hot gas is unable to feed the BH. Our model luminosity function therefore over-predicts the number of bright quasars at low redshift. However, our luminosity function correctly describes the density of quasars at $z \sim 1$ below the break in the luminosity function. This luminosity regime corresponds to most of the BH mass range in the locally observed $M_{\text{bh}} - M_{\text{halo}}$ relation. In order to match the bright end of the observed galaxy luminosity function, the infall of gas into galaxies with $v_c \gtrsim 500 \text{ km s}^{-1}$ must be suppressed (Kauffmann & Haehnelt 2000). This scale indeed corresponds to the cut-off in the v_c distribution of galaxies (Sheth et al. 2003). The dotted lines show the luminosity of a BH within a galaxy of mass $M_{\text{halo}} \sim 10^{13.5}$ corresponding to a circular

velocity of $\sim 500 \text{ km s}^{-1}$ at $z = 0$. This scale is close to the break in the quasar luminosity function at low-redshifts.

Near the peak of quasar activity at redshifts of $z \sim 2\text{--}3$ our model predicts a quasar lifetime of $t_{\text{dyn}} \sim 1\text{--}3 \times 10^7$ years. This result naturally explains observational estimates of quasar lifetimes (e.g Steidel et al. 2002; Yu & Tremaine 2002; Haiman & Hui 2001; Martini & Weinberg 2001). It is important to note that our model suggests that the observed lifetime is typical of quasars near the peak of the luminosity function, but that quasars at higher redshift have shorter lifetimes.

At redshifts below the peak of quasar activity our model successfully describes the luminosity function at luminosities fainter than the break (the agreement of the slope is particularly good). Boyle et al. (2000) found that the luminosity function at $z \lesssim 2.5$ is well described by a luminosity evolution. However inspection of Fig. 1 suggests that the evolution of quasars does not follow a luminosity evolution at high redshifts. In particular, our model suggests that rather than being an intrinsic feature of the quasars themselves, the break in the luminosity function is present only at low redshift and is a product of the inability of gas to cool inside massive dark matter halos. We also see that the faint end slope (reproduced at low redshift) evolves, becoming steeper at high redshift.

We emphasize that the redshift dependence of $M_{\text{bh}} \propto (1+z)^{5/2}$ in equation (4) is necessary to explain the density of bright quasars at $z \sim 6$. If the characteristic feedback time was constant, so that $M_{\text{bh}} \propto (1+z)$ as is the case for stars (see §3), then the sharp decline in the Press-

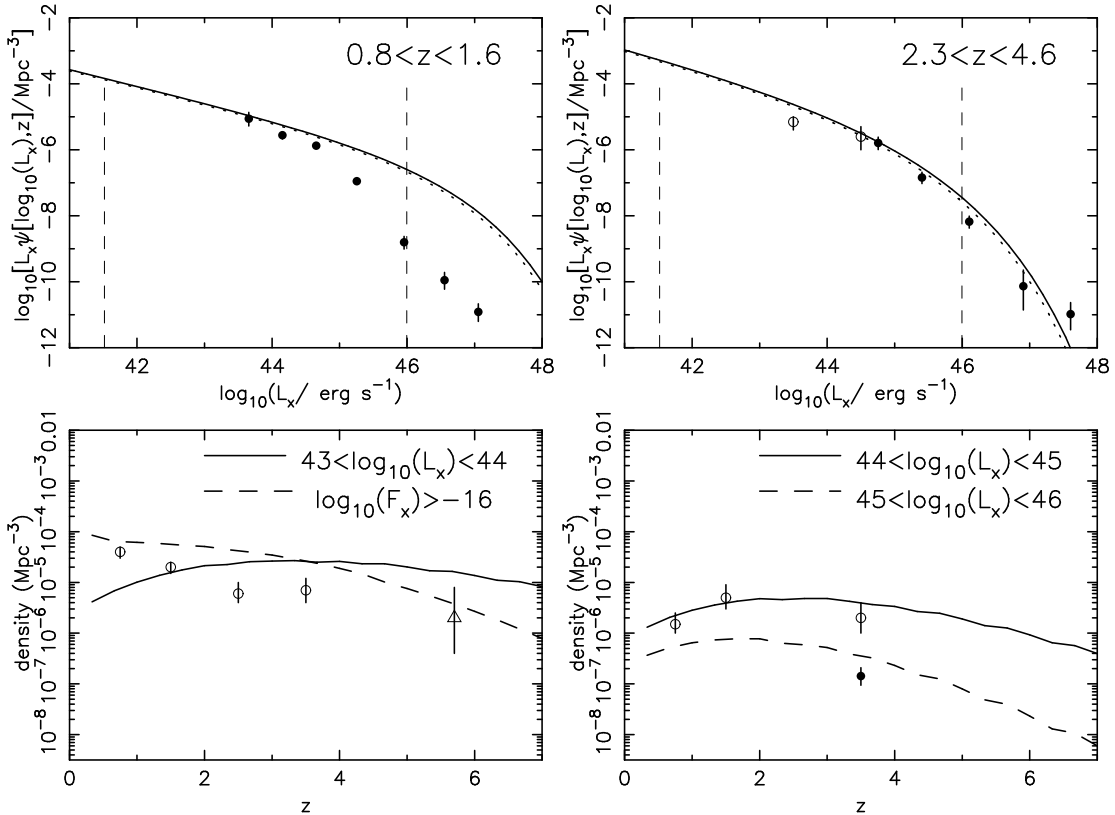


FIG. 2.— Upper panels: Comparison of the observed and model X-ray luminosity functions. In each panel the vertical dashed lines correspond to the Eddington luminosities of BHs bracketing the observed range of the $M_{\text{bh}}-v_c$ relation. Lower panels: evolution of the luminosity function with redshift in different luminosity ranges. The filled data points are from the luminosity function of Miyaji et al. (2001), while the open circles show results from Barger et al. (2003).

Schechter (1974) mass function with increasing halo mass would have resulted in a deficit of luminous quasars that cannot be compensated for by arbitrarily long quasar lifetimes. For example we find that the predicted density of quasars at $z \sim 2-3$ can be made consistent with observations by using a quasar lifetime of 10^8 years, but that the quasar abundance at $z \sim 6$ is underestimated by ~ 4 orders of magnitude.

The success of our model is particularly impressive, given the fact that its only free parameter (ηF_q) is directly set by local observations of BH masses, and that it assumes only that BH growth in a galactic disk is self regulating. In the following section, we demonstrate that this success extends into the X-ray regime.

3.2. The X-ray luminosity function

Haiman & Loeb (1999) noted that the luminosity function of quasars in the X-ray band at $z \sim 3$ can be related to the B-band luminosity function at that redshift if the median quasar spectral energy distribution is universal (Elvis 1994). They then extrapolated their model to predict the number counts of $z > 5$ quasars and found that ~ 50 should be detected in a *Chandra* deep field. Barger et al. (2002) have since found one $z > 5$ quasar in a circle of radius $6'$ at a flux level $F_X > 2 \times 10^{-16}$ erg s^{-1} . The new constraints provided by these very high redshift X-ray quasars (as well as optical high redshift quasars) motivate us to revisit the issue of modeling the X-ray luminosity function.

The number counts of X-ray quasars provide strong additional constraints on models of the luminosity function. At high luminosities, wide field surveys by the ROSAT satellite provide the X-ray luminosity function in the same luminosity range as the optical luminosity function. Therefore at $z \sim 3$, the comparison of the model optical and X-ray luminosity functions with the respective data sets tests the applicability of the median quasar spectrum adopted for the modeling (Haiman & Loeb 1999). However the deep X-ray surveys now becoming available (Cowie et al. 2002; Barger et al. 2003) probe bolometric quasar luminosities at $z \sim 3-5$ that are ~ 2 orders of magnitude fainter than are probed in the optical. This large dynamic range in luminosities provides a long lever arm for testing models of quasar evolution.

We follow Haiman & Loeb (1999) and construct the X-ray luminosity function in analogy with the B-band luminosity function using the median quasar spectrum of Elvis (1994). The universality of the spectrum is supported by the latest X-ray data on high redshift quasars (Brandt et al. 2002; Vignali et al. 2003). In order to facilitate comparison with observed luminosity functions we compute the luminosity L_{2-8} in an (intrinsic) X-ray band (e.g. 2–8keV) by integrating over the median spectrum. In analogy with equation (12) we find

$$\Psi(L_{2-8}, z) = \int_{0.25M_{\text{halo}}}^{0.5M_{\text{halo}}} dM_{\text{halo}} \frac{3}{5\epsilon} \frac{t_q}{L_{2-8, \odot}}$$

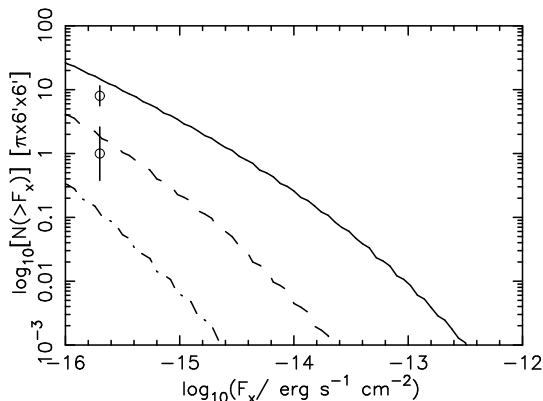


FIG. 3.— Number counts of quasars in a circle of radius $6'$ and redshifts above 3, 5 and 7 (top to bottom) as a function of the flux limit. The number counts from Barger et al. (2003) at $z > 3$ and $z > 5$ with flux $> 2 \times 10^{-16} \text{ erg s}^{-1} \text{ cm}^{-2}$ are shown for comparison.

$$\times \left. \frac{dn_{\text{ps}}}{dM} \right|_{M=M_{\text{halo}}-\Delta M_{\text{halo}}} \left. \frac{d^2 N_{\text{merge}}}{d\Delta M_{\text{halo}} dt} \right|_{M_{\text{halo}}-\Delta M_{\text{halo}}} \quad (12)$$

Here $L_{2-8, \odot} = \int_{2\text{keV}}^{8\text{keV}} dE_{\nu} \nu L_{\nu, \odot}$, where $\nu L_{\nu, \odot}$ is the spectral energy distribution of a solar mass BH radiating at its Eddington limit and $E_{\nu} = h\nu$ is the photon energy.

In the upper two panels of Fig. 2 we show the predicted X-ray luminosity function in the 0.5keV-2keV band (solid lines), and compare it with the observed luminosity function derived by Miyaji et al. (2001) from ROSAT data (solid dots). Luminosity functions (solid lines) are shown at $z \sim 1$ and $z \sim 3.5$. The bolometric luminosities of the observed quasars are comparable with those of bright optical quasars. We also show results (open circles) for lower luminosity X-ray AGN (Cowie et al. 2002; Barger et al. 2003). These luminosities refer to the 2–8keV range and should be compared to the dotted luminosity function. Several features of the comparison are similar to those of the optical luminosity function. The agreement is excellent at redshifts above the peak in quasar activity. However there is again an overproduction of bright quasars at $z \lesssim 2$, although the luminosity function below the break is reproduced. The interpretation of these features was discussed in the previous section. As noted by Haiman & Loeb (1999) the success of the model in producing both the optical and X-ray quasar luminosity functions at $z \gtrsim 2$ indicates that the median quasar spectral energy distribution is also a good representation at high redshifts. To help with the orientation between the optical (Haiman & Loeb 1998) and X-ray luminosity functions, we have placed vertical dashed lines at luminosities corresponding to the limits of the observed range of locally observed BH masses.

In the lower two panels of Fig. 2 we show the predicted density of X-ray quasars (solid lines) of different luminosities as a function of redshift in the 2keV-8keV band. These are compared with the observed densities derived by Cowie et al. (2002) and Barger et al. (2003) at low luminosities (open circles) and Miyaji et al. (2001) at higher luminosities (solid dots). At 10^{43} – $10^{44} \text{ erg s}^{-1}$, the model under predicts the quasar density at $z < 1$. However at luminosities of 10^{44} – $10^{45} \text{ erg s}^{-1}$, the observed redshift evolution is well described by our model.

We also compute the number counts of X-ray quasars. Barger et al. (2003) and Cowie et al. (2002) have recently

presented number counts of faint, high redshift quasars in the *Chandra* deep field north. The observations were made in the 0.4–6keV (observed) band and the minimum flux level was $2 \times 10^{-16} \text{ erg s}^{-1} \text{ cm}^{-2}$. We compute the comoving density of quasars with observed fluxes above this level in this band as a function of redshift by finding the luminosity function in the band $0.4(1+z)$ – $6(1+z)$ keV. This density is shown as the dashed line in the lower left panel of Fig. 2, along with the density at $z \sim 5.7$ corresponding to the observation of one quasar in the redshift range 5–6.5 within a circle of radius $6'$ (open triangle). The model is in agreement with the observation of one source at $z > 5$.

3.3. Number counts of high redshift X-ray quasars

We can also compute the number counts of high redshift X-ray quasars in the *Chandra* deep field north. Fig. 3 shows the number of quasars expected from the model with redshifts above 3, 5 and 7, and within a circle of radius $6'$ as a function of the flux limit. These are compared with the number counts from Barger et al. (2003) at $z > 3$ and $z > 5$. We find that ~ 1 –2 quasars with $z > 5$ and flux $> 2 \times 10^{-16} \text{ erg s}^{-1} \text{ cm}^{-2}$ are expected in the *Chandra* deep field north compared with the one observed. Similarly ~ 10 quasars with $z > 3$ and flux $> 2 \times 10^{-16} \text{ erg s}^{-1} \text{ cm}^{-2}$ are expected compared with 9 observed. This reproduction of the high redshift, low luminosity number counts is an impressive success of our model. For example, the Haiman & Loeb (1999) model, which postulated a linear relation of $M_{\text{bh}} \propto M_{\text{halo}}$, fails this test.

Motivated by this success we can use the model to predict the number counts of X-ray quasars at even higher redshifts. For example the results of Fig. 3 suggest that 0.1 quasar at $z > 7$ would be found in the *Chandra* deep field (or one quasar per 10 fields). Alternatively, probing deeper by a factor of ~ 3 in flux should allow detection of one quasar with $z > 7$ per field.

3.4. Using X-ray quasars to extend the optical luminosity function at high redshift to lower luminosities

The high redshift X-ray quasars discovered in the *Chandra* deep field have bolometric luminosities that are 2 orders of magnitude lower than the bright optically selected quasars. Using the median spectrum we can translate the

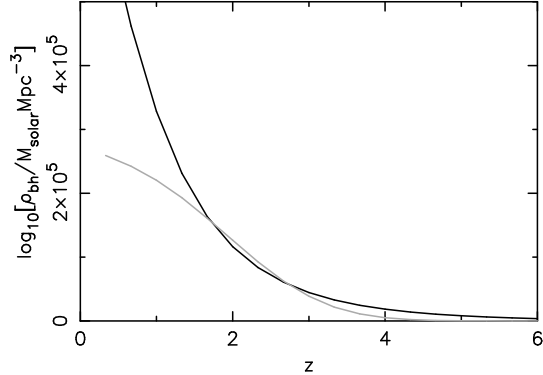


FIG. 4.— The mass density in supermassive BHs as a function of redshift for the luminosity function computed in this paper (dark line), and for the 2dF luminosity function (light line; Boyle et al. 2000).

density of X-ray quasars to points on the optical luminosity function. In the $2.5 < z < 3.5$ and $z \sim 4.3$ panels of Fig. 1 we plot the density of quasars with X-ray luminosities between $10^{43} - 10^{44} \text{ erg s}^{-1}$ and $10^{43} - 10^{44} \text{ erg s}^{-1}$, and $3 \lesssim z \lesssim 5$ in units of density per B-band luminosity (open circles) for comparison with the model optical quasar luminosity function. In the $z \sim 6$ panel we plot the density corresponding to one quasar per natural logarithm of luminosity in the redshift range $5 \lesssim z \lesssim 6.5$. The agreement is again excellent since the comparison simply presents the same data in a different way. However the comparison demonstrates agreement between model and data over a large range of luminosities at high redshift. In particular, it extends the comparison between model and data to the lower logarithmic half of the observed range of BH masses. At $z \sim 4.3$ the model produces the normalization and slope of the SDSS luminosity function, then becomes less steep at lower luminosities, and intersects the point computed from the X-ray observations, some 2.5 orders of magnitude away in luminosity (and therefore BH mass) and 2.5 orders of magnitude away in density per logarithm of luminosity. Similarly, the model satisfies the normalization of the luminosity function at $z \sim 6$ for both the low and high luminosity quasars as well as the constraint on the slope of the bright end of the luminosity function. The model also reproduces the suggestion from the data that the density of quasars changes more rapidly at high luminosities between $z \sim 4.3$ and $z \sim 6$.

4. ACCRETION OF BLACK-HOLE MASS DURING LUMINOUS PHASES

The comoving mass density accumulated by quasar BHs by a redshift z is

$$\rho_{\text{bh}}(z) = \int_z^\infty dz' \int_0^\infty dL_B \frac{L_{\text{bol}}}{\epsilon_{\text{rad}} c^2} \Psi(L_B, z') \frac{dt}{dz}, \quad (13)$$

where L_{bol} is the bolometric luminosity of a quasar with B-band luminosity L_B , and ϵ_{rad} is the efficiency of conversion of accreted mass to radiation. We take $\epsilon_{\text{rad}} = 0.06$, appropriate for the last stable orbit of a thin disk accretion onto a Schwarzschild BH. In Fig. 4 we show the mass density as a function of redshift for the luminosity function computed in this paper (dark line), and for the 2dF luminosity function (light line; Boyle et al. 2000). We find that $\rho_{\text{bh}} \sim 2 \times 10^5 M_\odot \text{Mpc}^{-3}$ has been accreted by $z \sim 1.5$, similar to estimations of the local BH density (e.g. Yu &

Tremaine 2002; Aller & Richstone 2002). Our luminosity function model erroneously indicates that growth continues at $z < 1.5$ due to the overestimate of massive galaxies at low redshift. As discussed in the analysis of Yu & Tremaine (2002), we find that an appreciable fraction of the present mass density in supermassive BHs is not accreted until after $z \sim 3$. Yu & Tremaine (2002) also find that $\sim 90\%$ of the present-day BH mass density is accreted before $z \sim 1.5$. Indeed, our luminosity function suggests that the accreted mass-density at $z \sim 1.5$ is comparable to the local value, and in agreement with the estimate from the 2dF luminosity function. We reiterate the point that by $z \sim 2 t_{\text{dyn}}$ is becoming comparable to the Salpeter time. Within the scheme outlined in this paper, that is the reason why most quasar growth occurs during this period. We therefore suggest that it is the feedback regulated accretion around the time of the peak in quasar activity that shapes the $M_{\text{bh}} - M_{\text{halo}}$ relation.

5. THE LOCAL MASS FUNCTION OF MASSIVE BLACK-HOLES

The local density of supermassive BHs can be computed by combining the $M_{\text{bh}} - \sigma$ relation with the velocity function of galaxies (e.g. Yu & Tremaine 2002; Aller & Richstone 2002). Until recently the velocity function had to be computed through combination of a galaxy luminosity function with the Faber-Jackson (1976) and Tully-Fisher (1977) relations. A more reliable representation is now possible using the measured velocity dispersion function of early type galaxies. Sheth et al. (2003) presented the measured velocity dispersion function for early type galaxies (which contain the most massive BHs), as well as a model for the velocity dispersion function of late-type galaxies. They suggested an analytic fit of the form

$$\phi(\sigma) d\sigma = \phi_* \left(\frac{\sigma}{\sigma_*} \right)^\alpha \frac{\exp[-(\sigma/\sigma_*)^\beta]}{\Gamma(\alpha/\beta)} \beta \frac{d\sigma}{\sigma}, \quad (14)$$

where ϕ_* is the number density of galaxies and σ_* is a characteristic velocity dispersion. Sheth et al. (2003) found that the parameters σ_* , α and β are strongly correlated with one another. We take $\phi_* = (2.0 \pm 0.1) \times 10^{-3} \text{Mpc}^{-3}$, $\alpha = 6.5 \pm 1.0$, $\beta = (14.75/\alpha)^{0.8}$ and $\sigma_* = 161 \Gamma(\alpha/\beta) / \Gamma[(\alpha+1)/\beta] \text{ km s}^{-1}$. From Fig. 6 in Sheth et al. (2003) we model the velocity dispersion function in the regime below $\sigma \sim 200 \text{ km s}^{-1}$ (where it is dominated by

late-type galaxies and measurements are not provided by SDSS) using the functional form

$$\phi(\sigma)d\sigma = \log_{10}(e) \times 10^{1.73-1.71\log_{10}(\sigma)} \frac{d\sigma}{\sigma}. \quad (15)$$

To compute the mass function of BHs, we combine $\phi(\sigma)$ with the $M_{\text{bh}} - \sigma$ relation

$$M_{\text{bh}} = M_{\text{bh},200} \left(\frac{\sigma}{200 \text{ km s}^{-1}} \right)^\chi. \quad (16)$$

Merritt & Ferrarese (2001) quote $M_{\text{bh},200} = (1.48 \pm 0.24) \times 10^8 M_\odot$ and $\chi = 4.65 \pm 0.48$. We computed a large number of realizations assuming that the parameters ϕ_* , α , $M_{\text{bh},200}$ and χ are distributed as Gaussian within their quoted uncertainties. We then find the mean and variance of the logarithm of the resulting set of mass functions.

In Fig. 5 we show the range (\pm twice the variance) in the computed mass function of BHs (solid area). This area is truncated below the region corresponding to the measured minimum density and the maximum measured velocity bin. The grey lines show the extrapolation to lower densities. The derived BH mass function differs substantially from that described in Aller & Richstone (2002). In particular, the cutoff at the high mass end is not as sharp in the present case. The reason is that the observed velocity function does not agree with that derived from the galaxy luminosity function and the Faber-Jackson relation (for a discussion, see Sheth et al. 2003).

We have computed the local mass-density in BHs by integrating the BH mass-function. We find a local BH density of $\rho_{\text{bh}} = (2.3_{-1.5}^{+4.0}) \times 10^5 M_\odot \text{Mpc}^{-3}$, where the quoted error is the density computed from mass-functions at the boundaries of the range shown in Fig. 5. Using the alternative values of $M_{\text{bh},200} = 1.14 \times 10^{8.13 \pm 0.06}$ and $\chi = 4.02 \pm 0.32$ (Tremaine et al. (2002) we find $\rho_{\text{bh}} \sim (2.5_{-1.7}^{+4.0}) \times 10^5 M_\odot \text{Mpc}^{-3}$. These estimates of BH density agree with the estimate of mass accreted during luminous quasar phases as described by the 2dF luminosity function (§ 4).

The local BH mass function may be compared with the redshift dependent mass function derived by combining the Press-Schechter (1974) mass function with the $M_{\text{bh}} - M_{\text{halo}}$ relation (4). We have plotted the resulting mass function at $z = 1, 3$ and 6 in Fig. 5. We find that the local density of BHs with masses below $M_{\text{bh}} \sim 10^8 M_\odot$ were in place by $z \sim 1 - 3$, coinciding with the peak in the quasar activity. More massive BHs were in place at even higher redshifts. In particular, we find that the most massive BHs known ($M_{\text{bh}} \sim 3 \times 10^9 M_\odot$) may have been in place by $z \sim 6$. This finding is in agreement with the conclusion of Loeb & Peebles (2003) that stars in giant ellipticals have already formed and expelled the surrounding gas at $z \sim 6$, but here the conclusion is derived from a completely independent argument.

5.1. The nearest very massive black-holes

Consider a BH of mass $M_{\text{bh}} \sim 3 \times 10^9 M_\odot$. We can estimate the co-moving density of black-holes directly from the observed quasar luminosity function and our estimate of quasar lifetime. At the peak of quasar activity, quasars powered by $M_{\text{bh}} \sim 3 \times 10^9 M_\odot$ BHs had a comoving density of $\Psi(> L) \sim 50 \text{Gpc}^{-3}$. However $t_{\text{Hubble}}/t_{\text{dyn}} \sim 2 \times 10^2$, so that the comoving density of BHs was $\sim 10^4 \text{Gpc}^{-3}$. As

this corresponds to the peak of BH growth, the BH density should match the value observed today. The density implies that the nearest BH of $\sim 3 \times 10^9 M_\odot$ should be at a distance $d_{\text{bh}} \sim (4\pi/3 \times 10^4)^{1/3} \text{Gpc} \sim 30 \text{Mpc}$ which is comparable to the distance of M87, a galaxy known to possess a BH of this mass (Ford et al. 1994).

What is the most massive BH that can be detected dynamically in a local galaxy redshift survey? The Sloan Digital Sky Survey probes a volume of $\sim 1 \text{Gpc}^3$ out to a distance ~ 30 times that of M87. At the peak of quasar activity, the density of the brightest quasars implies that there should be ~ 100 BHs with masses of $3 \times 10^{10} M_\odot$ per Gpc^3 , the nearest of which will be at a distance $d_{\text{bh}} \sim 130 \text{Mpc}$, or ~ 5 times the distance to M87. The radius of gravitational influence of the BH scales as $M_{\text{bh}}/v_c^2 \propto M_{\text{bh}}^{3/5}$. We find that for the nearest $3 \times 10^9 M_\odot$ and $3 \times 10^{10} M_\odot$ BHs, the angular radius of influence should be similar. Thus the dynamical signature of $\sim 3 \times 10^{10} M_\odot$ BHs on their stellar host should be detectable.

The luminosities of the brightest quasars at $z \sim 2-3$ imply BH masses of $\sim 10^{10} M_\odot$, even if they accrete at their Eddington rate. The masses could be lower if the emission is beamed, though this does not appear to be the case for high redshift quasars (e.g. Willott, McLure & Jarvis 2003). The implied density of $\sim 10^{10} M_\odot$ BHs is in excess of the densities obtained by convolving the galaxy velocity function (Sheth et al. 2003) with the $M_{\text{bh}} - \sigma$ relation (Merritt & Ferrarese 2001; Tremaine et al. 2002). This is shown by the dot-dashed lines in Fig. 5. Here we have estimated the density of black-holes as implied by the quasar luminosity function at $z \sim 2.3$ and $z \sim 3$ according to

$$\frac{d\Psi_{\text{bh}}}{dM_{\text{bh}}} = \frac{t_q}{H^{-1}} \frac{dL}{dM_{\text{bh}}} \Psi(L), \quad (17)$$

where we have used $dM_{\text{bh}} = dL/5.73 \times 10^3$. The presence of these BHs at $z \sim 2 - 3$ may imply that these very massive BHs will be found in the central galaxies of large clusters of galaxies.

6. REGULATION OF STAR FORMATION

We may derive the limiting stellar mass of a galaxy in view of the same self-regulation principle (Dekel & Woo 2002). Suppose that stars form with an efficiency f_* out of the gas that collapses and cools within a dark-matter halo, and that a fraction F_{SN} of each supernova energy output, E_{SN} , heats the galactic gas mechanically. The mechanical feedback will halt the star formation once the cumulative energy returned to the gas by supernovae equals its binding energy (assuming negligible radiative losses for a sufficiently rapid starburst). Hence the limiting stellar mass is set by the condition,

$$\frac{M_*}{w_{\text{SN}}} E_{\text{SN}} F_{\text{SN}} = E_b = \frac{1}{2} \frac{\Omega_b}{\Omega_m} M_{\text{halo}} v_c^2, \quad (18)$$

where w_{SN} is the mass in stars (in M_\odot) per supernova explosion. Equation (18) implies that the total mass in stars, $M_* = (f_* \Omega_b / \Omega_m) M_{\text{halo}}$, scales as

$$M_* \propto M_{\text{halo}}^{5/3} [\xi(z)]^{1/3} (1+z). \quad (19)$$

At a fixed redshift, the star formation efficiency scales as $f_* \propto v_c^2 \propto M_{\text{halo}}^{2/3}$. Thus smaller galaxies are less efficient at

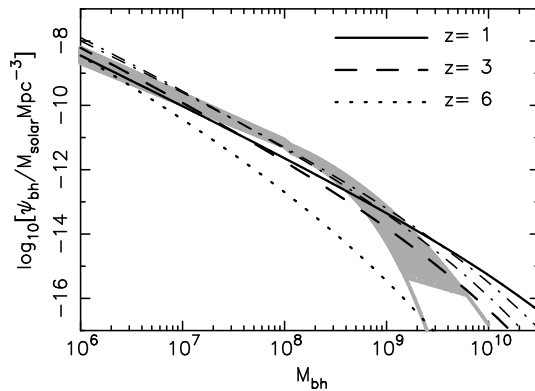


FIG. 5.— The mass function of supermassive BHs. The grey region shows the mass function estimated from the velocity function of Sheth et al. (2003) and the $M_{\text{bh}} - \sigma$ relation of Merritt & Ferrarese (2001). The lower bound corresponds to the lower limit in density for the observed velocity function ($\sigma \frac{d\Phi}{d\sigma} > 10^{-6.2}$), while the grey lines show the extrapolation to lower densities. We also show the mass function computed at $z = 1, 3$ and 6 from the Press-Schechter (1974) halo mass function and equation (4), as well as the mass function at $z \sim 2.35$ and $z \sim 3$ implied by the observed density of quasars and a quasar lifetime t_{dyn} (dot-dashed lines).

forming stars, but a galaxy of fixed mass is more efficient at higher redshift. A Scalo (1986) mass function of stars has $w_{\text{SN}} = 126 M_{\odot}$ per supernova and $E_{\text{SN}} = 10^{51}$ ergs, and so we find that a mass in stars of $M_{\star} = 3 \times 10^{10} M_{\odot}$ and a velocity of $v_c \sim 175 \text{ km s}^{-1}$ [the typical value observed locally (Bell & De Jong 2001)] implies $F_{\text{SN}} \sim 0.5$ and $f_{\star} = 0.07$. The star formation efficiency in the most massive spiral galaxies is therefore expected to be $\sim 10\%$.

7. REDSHIFT DEPENDENCE OF THE MAGORRIAN ET AL. (1998) RELATION

In the preceding sections we have found that the mass of BHs scales as v_c^5 while the star formation efficiency scales as v_c^2 . This is because the luminosity of a quasar is limited by the Eddington value and is proportional to the BH mass, while the energy release rate of supernovae is proportional to the total stellar mass. Hence we find that the ratio of BH to stellar mass,

$$\frac{M_{\text{bh}}}{M_{\star}} \propto [\xi(z)]^{\frac{1}{2}} (1+z)^{\frac{3}{2}}, \quad (20)$$

is independent of mass as observed (Magorrian et al. 1998). However, we find that the relation evolves with redshift, and that the BH comprises a larger fraction of the stellar mass at a higher redshift. This effect has been seen in a sample of gravitationally lensed quasars (with lensed host galaxies); Rix et al. (1999) found that host galaxies are much fainter at $z \sim 2$ when compared with lower redshift galaxies containing quasars of comparable luminosity. Our results are also consistent with the semi-analytic predictions of Kauffmann & Haehnelt (2000).

8. COMPARISON WITH PREVIOUS WORK

Since the work by Haehnelt, Natarajan & Rees (1998) there have been several attempts to describe the quasar luminosity function within hierarchical merging scenarios through semi-analytic modeling. Kauffmann & Haehnelt (2000) assumed that the $M_{\text{bh}} - \sigma$ relation was set by the amount of gas that cools and becomes available for star formation. They found that they could explain the decrease in quasar activity at low redshift based on the decrease in merger rates, the decrease in the gas available to fuel BHs, and the assumption that gas accretes more

slowly at late times. For an accretion timescale that scales as $(1+z)^{-3/2}$, these considerations led to quasar hosts that are a factor of 10 less massive at $z \sim 2$ than in the local universe. Volonteri, Haardt & Madau (2002) followed the evolution of the BH population through a merger-tree algorithm. They modeled the luminosity function by fixing the $M_{\text{bh}} - \sigma$ relation from observations, and forcing the quasar lifetime following a merger to be equal to the time for accretion of the mass to match the $M_{\text{bh}} - \sigma$ relation at an efficiency of 10%.

Di Matteo, Croft, Springel & Hernquist (2003) noted that the above studies either assume the $M_{\text{bh}} - \sigma$ relation from observations, or derive it based on additional assumptions. They suggested that a linear relationship between the gas in bulges and M_{bh} results in the local $M_{\text{bh}} - \sigma$ relation, the drop in quasar density at low redshift, and the regulation of BH growth through supernovae feedback. However their model over-predicts the density of high-redshift quasars. In their conclusion, Di Matteo et al. (2003) state that it seems unlikely that BH accretion affects gas dynamics in galaxies unless feedback from the quasar itself is important. On the other hand, the importance of quasar feedback has recently been highlighted by Begelman (2003).

In the previous sections, we have demonstrated that a scenario in which quasar feedback limits BH growth through regulation of the quasar lifetime naturally reproduces the quasar luminosity function at high redshifts. For the first time we have compared the model to both the $z \sim 6$ SDSS luminosity function and the X-ray luminosity function, allowing comparison over ~ 3 orders of magnitude in flux and 3 orders of magnitude in quasar density per logarithmic luminosity interval at $z > 5$. The success of the model signals several important implications. First, around the peak of quasar activity at $z \sim 2.5$ the quasar lifetime, interpreted here as the dynamical time of the host galactic disk, is $\sim 10^7$ years [see Eq. (7)]. This provides a natural explanation for observational estimates of the lifetime (e.g. Steidel et al. 2002; Yu & Tremaine 2002). Moreover, the dynamical time of the disk becomes comparable to the Salpeter growth time at this redshift, so that most of the mass in a given BH was added during

this epoch. Thus we suggest that the growth of BHs during luminous quasar phases around this time, regulated by feedback from the quasar itself, set the slope and amplitude of the the $M_{\text{bh}} - v_c$ relation observed today.

9. CONCLUSIONS

We have shown that if BHs grow in the centers of galaxies until they unbind the galactic gas that feeds them over a dynamical time, then the locally observed relation between BH mass and halo velocity dispersion (Ferrarese 2002) is recovered both in slope and normalization. We include this feedback regulation of BH growth in a model of the quasar luminosity function and find that the observed optical quasar luminosity function at $z \gtrsim 2$ as well as at luminosities below the break at lower redshifts, are reproduced for hierarchical merging of galactic halos in the standard Λ CDM cosmology. Moreover, using the median quasar spectral energy distribution we showed that the same model yields good agreement with the X-ray quasar luminosity function at $z \gtrsim 2$ (and the luminosity function below the break at lower redshifts). The model suggests that ~ 10 faint quasars at $z > 3$ and ~ 1 at $z > 5$ should have been found in the *Chandra* deep field north at a flux above 2×10^{-16} erg s $^{-1}$ cm $^{-2}$, in agreement with the observed number counts. Overall, the model describes observations of the high redshift luminosity function over ~ 3 orders of magnitude in bolometric luminosity and ~ 3 orders of magnitude in comoving density per logarithm of luminosity. This success is impressive given the fact that the model is based on a simple algorithm with only one adjustable parameter, namely the

quasar feedback power in Eddington units ηF_q , and that this quantity is set by local observations of BH masses. Our model associates the inferred quasar lifetime of $\sim 10^7$ years (Steidel et al. 2002) with the dynamical time of a galactic disk during the peak of quasar population ($z \sim 2-3$). Moreover, since the quasar lifetime is comparable to the Salpeter time during this epoch, the model suggests that the slope and normalization of the locally observed $M_{\text{bh}} - M_{\text{halo}}$ relation resulted from feedback regulated accretion around this epoch. We have computed the local mass-function of BHs by combining the $M_{\text{bh}} - \sigma$ relation with the measured velocity dispersion function of Sheth et al. (2003). Comparison of the local BH mass function with the mass function inferred from the feedback relation and halo mass-function implies that the most massive galaxies already hosted their present-day BHs by $z \sim 3-6$ (see also Loeb & Peebles 2003). Finally, we showed that if supernova feedback regulates star formation in a similar way, then the Magorrian et al. (1998) relation between the BH and stellar masses of galactic spheroids should be redshift dependent [see Eq. (20)], as observed for the hosts of gravitationally lensed quasars (Rix et al. 1999).

JSBW thanks the Institute for Advanced Study for its pleasant hospitality during the course of this work. AL acknowledges support from the Institute for Advanced Study and the John Simon Guggenheim Memorial Fellowship. This work was also supported in part by NSF grants AST-0071019, AST-0204514 and NASA grant ATP02-0004-0093.

REFERENCES

- Aller, M.C., Richstone, D.O., 2002, astro-ph/0210573
 Baes, M., Buyle, P., Hau, G.K.T. & Dejonghe, H., 2003, astro-ph/0303628
 Barger, A. J., Cowie, L. L., Capak, P., Alexander, D. M., Bauer, F. E., Brandt, W. N., Garmire, G. P., & Hornschemeier, A. E. 2003, astro-ph/0301232
 Barkana, R., & Loeb, A. 2001, Phys. Rep., 349, 125-238
 Begelman, M.C., 2003, astro-ph/0303040
 Bell, E. F. & de Jong, R. S. 2001, ApJ, 550, 212
 Bennett, C. L., et al. 2003, ApJ, submitted; astro-ph/0302207
 Boyle, B. J., Shanks, T., Croom, S. M., Smith, R. J., Miller, L., Loaring, N., & Heymans, C. 2000, MNRAS, 317, 1014
 Brandt, W.N., et al., 2002, astro-ph/0212082
 Cowie, L. L., Barger, A. J., Bautz, M. W., Brandt, W. N., & Garmire, G. P. 2003, ApJ, 584, L57
 Dekel, A. & Woo, J. 2002, astro-ph/0210454
 Dekel, A. & Silk, J. 1986, ApJ, 303, 39
 Matteo, T. D., Croft, R. A. C., Springel, V., & Hernquist, L. 2003, astro-ph/0301586
 Elvis, M. et al. 1994, ApJS, 95, 1
 Faber, S. M. & Jackson, R. E. 1976, ApJ, 204, 668
 Fabian, A. C. 2003, to appear in "Carnegie Observatories Astrophysics Series, Vol. 1: Co-evolution of Black Holes and Galaxies," ed. L. C. Ho
 Fan, X., et al. 2001a AJ, 121, 54
 Fan, X., et al. 2001b AJ, 122, 2833
 Fan, X., et al. 2003, astro-ph/0301135
 Ferrarese, L. 2002, ApJ, 578, 90
 Floyd, D.J.E., 2003, astro-ph/0303037
 Ford, H. C., et al. 1994, ApJ, 435, L27
 Furlanetto, S. R. & Loeb, A. 2001, ApJ, 556, 619
 Haehnelt, M.G., Natarajan, P., Rees, M.J. 1998, MNRAS, 300, 817
 Haiman, Z. & Hui, L. 2001, ApJ, 547, 27
 Haiman, Z. & Loeb, A. 1998, ApJ, 503, 505
 Haiman, Z. & Loeb, A. 1999, ApJ, 521, L9
 Hernquist, L., & Mihos, J.C. 1995, ApJ., 448, 41
 Kauffmann, G., & Haehnelt, M. 2000, MNRAS, 311, 576
 Lacey, C., & Cole, S. 1993, MNRAS, 262, 627
 Loeb, A., & Peebles, P. J. E. 2003, ApJ, in press; astro-ph/0211465
 Magorrian, J. et al. 1998, AJ, 115, 2285
 Martini, P. & Weinberg, D. H. 2001, ApJ, 547, 12
 Merritt, D., & Ferrarese, L., 2001, ApJ., 547, 140
 Mihos, J.C., & Hernquist, L. 1994, ApJ., 431, L9
 Miyaji, T., Hasinger, G., & Schmidt, M. 2001, A&A, 369, 49
 Mo, H. J., Mao, S., & White, S. D. M. 1998, MNRAS, 295, 319
 Pei, Y. C. 1995, ApJ, 438, 623
 Press, W. H., & Schechter, P. 1974, ApJ, 187, 425
 Rix, H.-W., et al., 1999, astro-ph/9910190
 Scalo, J. M. 1986, Fundamentals of Cosmic Physics, 11, 1
 Sheth, R. K., et al. 2003, ApJ, submitted; astro-ph/0303092
 Shields, G. A., Gebhardt, K., Salviander, S., Wills, B. J., Xie, B., Brotherton, M. S., Yuan, J., & Dietrich, M. 2003, ApJ, 583, 124
 Silk, J. & Rees, M. J. 1998, A&A, 331, L1
 Steidel, C. C., Hunt, M. P., Shapley, A. E., Adelberger, K. L., Pettini, M., Dickinson, M., & Giavalisco, M. 2002, ApJ, 576, 653
 Tremaine, S. et al. 2002, ApJ, 574, 740
 Tully, R. B. & Fisher, J. R. 1977, A&A, 54, 661
 Vignali, C., et al., 2003, astro-ph/0302558
 Volonteri, M., Haardt, F., & Madau, P. 2003, ApJ, 582, 559
 Willott, C. J., McLure, R. J., & Jarvis, M. J. 2003, astro-ph/0303062
 Wyithe, J. S. B. & Loeb, A. 2002, ApJ, 581, 886
 Yu, Q., & Tremaine, S. 2002, astro-ph/0203082